

1   **A robust and comprehensive quality control of cerebral cortical organoids: methodology and**  
2   **validation**

3   Héloïse Castiglione<sup>1, 2, 3, \*</sup>, Lucie Madrange<sup>1, 2</sup>, Camille Baquerre<sup>3</sup>, Benoît Guy Christian Maisonneuve<sup>3</sup>, Jean-  
4   Philippe Deslys<sup>2</sup>, Frank Yates<sup>1, 2</sup>, Thibault Honegger<sup>3</sup>, Jessica Rontard<sup>3, &</sup> and Pierre-Antoine Vigneron<sup>1, 2, &, \*</sup>

5

6   1: SupBiotech, Ecole d'Ingénieurs en Biotechnologies, Villejuif, France.

7   2: Université Paris-Saclay, Commissariat à l'Energie Atomique et aux Energies Alternatives (CEA), Service  
8   d'Etude des Prions et des Infections Atypiques (SEPIA), Fontenay-aux-Roses, France.

9   3: NETRI, Lyon, France.

10   &: Equal contributions

11   \*: Correspondence, [heloise.castiglione@netri.com](mailto:heloise.castiglione@netri.com) ; [pierre-antoine.vigneron@supbiotech.fr](mailto:pierre-antoine.vigneron@supbiotech.fr)

12

13   **ORCID**

14   Héloïse Castiglione: 0000-0002-7543-0836

15   Lucie Madrange: None

16   Camille Baquerre: None

17   Benoît Maisonneuve: 0000-0001-6961-3671

18   Jean-Philippe Deslys: None

19   Frank Yates: 0000-0002-3590-5745

20   Thibault Honegger: 0000-0002-1716-7363

21   Jessica Rontard: 0009-0008-9422-2339

22   Pierre-Antoine Vigneron: 0000-0003-2918-0909

23

24   **ACKNOWLEDGMENTS**

25   The authors would like to express their sincere gratitude to François Hémard for his contributions to the  
26   acquisition, processing, and analysis of γH2AX images, and to Axel Fontanier for his valuable help in brightfield  
27   image acquisition. Special thanks are extended to Thomas Lemonnier for his work on reprogramming the BJ  
28   fibroblast cell line into induced pluripotent stem cells and to Elise Delage for her expert guidance on image analysis  
29   and fluorescence quantification. Finally, we warmly thank Florian Laramandy for his review of the manuscript.

30 **ABSTRACT**

31 Cerebral organoids hold great promise for neuroscience research as complex *in vitro* models that mimic  
32 human brain development. However, they face significant challenges related to quality and reproducibility, leading  
33 to unreliability in both academic and industrial contexts. Discrepancies in morphology, size, cellular composition,  
34 and cytoarchitectural organization limit their application in biomedical studies, particularly in disease modeling,  
35 drug screening, and neurotoxicity testing, where consistent models are essential. Critically, current methods for  
36 organoid characterization often lack standardization and rely heavily on subjective assessments, restricting their  
37 broader applicability. In this study, we developed a comprehensive Quality Control (QC) framework for 60-days  
38 cortical organoids. Five key criteria: morphology, size and growth profile, cellular composition, cytoarchitectural  
39 organization, and cytotoxicity, are evaluated using a standardized scoring system. We implemented a hierarchical  
40 approach, beginning with non-invasive assessments to exclude low-quality organoids (Initial Scoring), while  
41 reserving in-depth analyses for those that passed the initial evaluation (Final Scoring). To validate this framework,  
42 we exposed 60-day cortical organoids to graded doses of hydrogen peroxide ( $H_2O_2$ ), inducing a spectrum of quality  
43 outcomes. The QC system demonstrated its robustness and reproducibility by accurately discriminating organoid  
44 quality based on objective and quantifiable metrics. This standardized and user-friendly framework for quality  
45 assessment not only minimizes observer bias but also enhances the reliability and comparability of cerebral  
46 organoid studies. Additionally, its scalability makes it suitable for industrial applications and adaptable to other  
47 organoid types, offering a valuable tool for advancing both fundamental and preclinical research.

48

49 **KEYWORDS:** Cerebral organoids, Quality Control, Hierarchical Scoring Methodology, Reproducibility,  
50 Standardization.

51

52 **INTRODUCTION**

53 Cerebral organoids have emerged as innovative tools in neuroscience by providing biologically relevant  
54 *in vitro* models that recapitulate aspects of the human brain development and function. These three-dimensional  
55 (3D) structures, derived from the neuroectodermal differentiation of pluripotent stem cells, self-organize into  
56 complex architectures recapitulating certain regions of the human brain [1], such as the forebrain, midbrain,  
57 hindbrain, or even more specifically the hippocampus, cortex, or choroid plexus [2–12]. Unspecific differentiation  
58 protocol can also give rise to unguided whole-brain organoids [13].

59 Unlike traditional 2D cultures or simpler 3D models such as spheroids and neurospheres, cerebral  
60 organoids recreate a physiologically relevant cellular microenvironment. This complexity allows for enhanced  
61 cell-cell and cell-matrix interactions, fostering improved differentiation and maturation [14]. While human brain  
62 organogenesis remains a highly complex process, tightly regulated both on a spatial and a temporal scale [15],  
63 cerebral organoids have proven their ability to model key neurodevelopmental aspects, including neurogenesis,  
64 neuronal migration, neuromorphogenesis and synaptogenesis [1, 15]. Furthermore, transcriptomic and epigenetic  
65 analyses have revealed that these models closely mimic developmental trajectories observed in the human fetal  
66 brain [15, 16]. When derived from patient-specific cells, or when combined with advanced genetic engineering  
67 techniques, such features have made cerebral organoids powerful tools for studying neurodevelopmental disorders,  
68 such as microcephaly [13] and trisomy 21 [17–19], as well as for studying neurological cancers [20], and can also  
69 give clues about the pathogenesis of neurodegenerative diseases, including Alzheimer’s disease [21, 22],  
70 Parkinson’s disease [23], and Creutzfeldt-Jakob disease [24].

71 Beyond modeling diseases, cerebral organoids have shown promise in neurotoxicity studies [25, 26].  
72 Notably, the developing human brain is highly susceptible to environmental insults, and exposure to pollutants or  
73 chemicals during pregnancy can disrupt its physiological development. Organoids could provide an unprecedented  
74 human-based predictive model to study developmental neurotoxicity (DNT) in response to drugs, chemicals, and  
75 pollutants. Studies using cerebral organoids have already explored the effects of valproic acid [27–34], nicotine  
76 [35], cannabis [36], bisphenols [37, 38], cadmium [39] and nanoplastics [40], among others [41–44].

77 Despite their potential, cerebral organoids face significant challenges in terms of quality and  
78 reproducibility. Morphological inconsistencies, variations in size, and differences in cellular composition or  
79 cytoarchitectural organization often arise from the stochastic nature of stem cell differentiation and the spontaneous

80 self-organization occurring within the organoid [1, 45]. For instance, within a batch of cerebral organoids, some  
81 organoids will display optimal morphology, with dense overall structure and well-defined borders, while others  
82 maybe poorly compact and will tend to degrade over time by losing cells [46, 47]. Moreover, some organoids will  
83 exhibit expected cell types and cytoarchitectural organization, whereas others may present disorganized structures  
84 and lower proportions of some cell types. Similarly, suboptimal cystic cavities can also be present within some  
85 organoids or protrude from their surface [46]. In addition, a necrotic core can also arise in certain organoids [1, 45,  
86 48]. Non-cerebral structures might also occasionally occur, including germ layers other than neuroectoderm,  
87 especially in the unguided-differentiated organoids [1, 49]. These inconsistencies compromise the reproducibility  
88 of scientific results, particularly in disease modeling, neurotoxicity testing, and preclinical drug screening, where  
89 high-quality and consistent models are essential [45]. Furthermore, the lack of standardized criteria for organoid  
90 generation, culture, and characterization exacerbates this variability, creating barriers to their broader adoption in  
91 industrial and preclinical applications.

92 Current methods for organoid characterization, including immunohistochemistry [2, 13], transcriptomic  
93 profiling [6], electrophysiological recording [50], and cytotoxicity studies [51–55] are valuable but often lack  
94 standardization and face several limitations. Many current approaches rely on qualitative and subjective  
95 assessments that might introduce inconsistencies and bias. It is common that for daily evaluation of cerebral  
96 organoids, researchers rely on morphological observations to assess quality, but this qualitative readout is not  
97 frequently detailed in research publications. Although morphological criteria are often used and provide valuable  
98 information, their translation into standardized quantitative indicators transferable between laboratories remains  
99 partially done, even if recent publications highlight a growing interest in leveraging these criteria as reliable, non-  
100 invasive readouts for characterizing cerebral organoids [56–58]. Moreover, some analysis methods commonly used  
101 in 2D cell cultures are difficult to transpose to 3D cultures, further complicating the standardization of their  
102 characterization [55, 59]. Overall, there is a notable lack of robust and well-defined quantitative methodologies  
103 for 3D organoid characterization. This gap limits the ability to objectively evaluate cerebral organoids in terms of  
104 quality, especially across diverse research groups, ultimately affecting the reliability and consistency of results.

105 In this study, we propose a comprehensive and robust Quality Control (QC) framework for 60-day cortical  
106 organoids to address these challenges in their evaluation. This system integrates five critical criteria: A)  
107 Morphology, B) Size and Growth Profile, C) Cellular Composition, D) Cytoarchitectural Organization, and E)  
108 Cytotoxicity, into a standardized scoring methodology. The framework is designed hierarchically, prioritizing  
109 early, non-invasive evaluations to efficiently exclude organoids of low quality, while reserving in-depth analyses  
110 for organoids that have met initial thresholds. To validate its reliability and applicability, we exposed 60-day  
111 cortical organoids to gradual doses of hydrogen peroxide ( $H_2O_2$ ), producing varying quality levels to rigorously  
112 test the scoring system. By minimizing observer bias and enabling objective, reproducible quality assessments,  
113 this QC framework enhances the consistency and comparability of results in cerebral organoid research. Moreover,  
114 its potential to support both academic studies and industrial scalability highlights its value as a versatile tool for  
115 advancing biomedical research.

116

## 117 MATERIALS AND METHODS

118 **hiPSC culture and maintenance** – Human induced Pluripotent Stem Cells (hiPSCs) were generated by  
119 reprogramming BJ primary foreskin fibroblasts obtained from ATCC (CRL-2522), using the non-integrative  
120 Sendai virus vectors following the manufacturer's instructions (A16517, ThermoFisher Scientific). Pluripotency  
121 was confirmed by identifying specific pluripotency markers through Reverse Transcriptase-Polymerase Chain  
122 Reaction (RT-PCR), and regular tests were conducted to verify the absence of mycoplasma. The culture and  
123 maintenance of hiPSCs were performed as previously reported [21, 22, 55]. Briefly, hiPSCs were maintained on  
124 Geltrex-coated cell culture plates (A1569601, Gibco) and cultured in mTeSR™ Plus medium (100-0276,  
125 STEMCELL Technologies) supplemented with 1% Penicillin/Streptomycin (P/S) (15140122, Gibco), at 37°C in a  
126 5%-enriched CO<sub>2</sub> atmosphere. hiPSCs were passaged upon reaching 50-70% confluence using 0.02%  
127 ethylenediaminetetraacetic acid (EDTA) treatment (E8008, Sigma-Aldrich).

128 **Generation and culture of cerebral cortical organoids** – Cerebral cortical organoids were generated as  
129 previously reported [55], from a protocol adapted from methods described by Xiang *et al.* [4, 5] relying on dorsal  
130 forebrain-regionalized differentiation. On day 0, hiPSCs were detached using 0.02% EDTA treatment and  
131 dissociated with Accutase (AT-104, STEMCELL Technologies) to obtain a single-cell suspension. These cells were

132 seeded in V-bottom cell-repellent 96-well plates (651970, Greiner Bio-One) at a density of 20,000 cells/well in  
133 neural induction medium containing Dulbecco's Modified Eagle Medium/Nutrient Mixture F-12, GlutaMAX  
134 supplement (DMEM/F-12, 10565018, Gibco), 15% (v/v) KnockOut Serum Replacement (KOSR, 10828010,  
135 Gibco), 1% Minimum Essential Medium-Non-Essential Amino Acids (MEM-NEAA, 1140035, Gibco), 1% P/S,  
136 100 nM LDN-193189 (72147, STEMCELL Technologies), 10 µM SB-431542 (72232, STEMCELL  
137 Technologies), 2 µM XAV-939 (X3004, Sigma-Aldrich), 100 µM β-mercaptoethanol (21985023, Gibco), and  
138 supplemented with 5% Fetal Bovine Serum (FBS, 10270106, Gibco) and 50 µM Y-27632 (72304, STEMCELL  
139 Technologies). On day 2, embryoid bodies (EBs) were collected and transferred into 24-well suspension cell  
140 culture plates (144530, Nunc). The neural induction medium was renewed every two days until day 10, with FBS  
141 removed from day 2, and Y-27632 removed from day 4. From day 10 to day 18, EBs were cultured in differentiation  
142 medium without vitamin A, containing DMEM/F-12:NeuroBasal Medium (21103049, Gibco) at 1:1 ratio,  
143 supplemented with 0.5% (v/v) MEM-NEAA, 1% P/S, 0.5% N2 supplement 100X (17502-048, Gibco), 1% B-27  
144 supplement minus vitamin A (12587010, Gibco), 1% HEPES solution (H0887, Sigma-Aldrich), 0.025% human  
145 insulin (19278-5 mL, Sigma-Aldrich), and 50 µM β-mercaptoethanol. From day 18, EBs were cultured in a  
146 differentiation medium with vitamin A, following the same composition as the previously described medium, but  
147 replacing the B-27 supplement minus vitamin A, with B-27 supplement with vitamin A (17504044, Gibco), and  
148 supplemented with 20 ng/mL BDNF (78005, STEMCELL Technologies), 200 µM ascorbic acid (A9290225G,  
149 Sigma-Aldrich), and 200 µM cAMP (73886, STEMCELL Technologies). Cortical organoids were cultured in 24-  
150 well plates with 500 µL of culture medium renewed every two days from day 2 to day 28. After day 28, the medium  
151 volume was increased to 1 mL and renewed once a week. Organoids were cultured under agitation (80 rpm/min)  
152 at 37°C, in a 5%-enriched CO<sub>2</sub> atmosphere.

153 **H<sub>2</sub>O<sub>2</sub> exposures on cortical organoids** – Cortical organoids were exposed on day 61 of culture to hydrogen  
154 peroxide (H<sub>2</sub>O<sub>2</sub>) (1.07209.0250, Supelco) diluted in differentiation medium with vitamin A, at several doses (0.1%,  
155 0.25%, 0.5%, 1% and 5%) during 30 min at 37°C. After exposure, cortical organoids were washed once with fresh  
156 culture medium to remove excess H<sub>2</sub>O<sub>2</sub>, were maintained in culture for 7 days, and were fixed on day 68.

157 **Quality Control of cortical organoids: scoring system** – A multi-criteria scoring system was developed for the  
158 QC of 60-day cortical organoids (Fig. 1 and Fig. S1). It is designed with criteria following a strict hierarchy, where  
159 the most critical ones are assessed first. If an organoid fails to meet the required score for an index, it is immediately  
160 excluded from further consideration (Fig. 1A). For the QC scoring, a detailed description (Fig. S1) outlines  
161 expected values and scoring thresholds for each index. Additionally, a summary table with the minimum scores  
162 required to pass the QC for each criterion is presented (Fig. 1B). Based on their individual QC scores obtained,  
163 cortical organoids are classified into “QC passed” or “QC failed” categories, with the specification of the failed  
164 scoring step for any organoid that did not pass the QC. More precisely, the scoring approach is tailored to be usable  
165 both for pre- and post-study, referred to as Initial QC and Final QC, respectively.

166 **Initial Quality Control** – In the pre-study phase, the first two non-invasive criteria, A (Morphology) and B (Size  
167 and Growth Profile), are evaluated across a batch of cortical organoids, to identify those suitable for inclusion in  
168 the subsequent study. The morphology of the organoids is assessed based on their color, density, compactness,  
169 border integrity, as well as depending on the absence or presence of cysts. In addition, organoid sizes and growth  
170 profiles are monitored to ensure they remain within expected growth ranges.

171 **Final Quality Control** – In the post-study phase, all five criteria – A to E – are used to thoroughly validate organoid  
172 quality. This includes additional evaluations of cellular populations (criterion C), where the presence of the three  
173 expected cell types (neurons, astrocytes, neural progenitors) and astrocytic reactivity are analyzed, as well as  
174 assessments of the cytoarchitectural organization (criterion D), including cell density, proportion of cell-less  
175 regions, border integrity, presence of neurogenic areas, and occurrence of internal cysts. Finally, cell viability and  
176 cytotoxic markers (criterion E) are evaluated, with a focus on DNA damage and apoptotic markers, to ensure  
177 organoids have maintained low cytotoxicity levels throughout the study.

178 **Longitudinal monitoring of cortical organoid morphology and growth evolution** – For cortical organoid  
179 morphology and growth profile monitoring over time, brightfield images of the organoids were acquired at regular  
180 timepoints during the culture (D+2, D+9, D+16, D+23, D+30, D+33, D+40, D+48, D+54 and D+61), using a DM  
181 IL LED Inverted Laboratory Microscope (Leica Microsystems) (5X). To assess the organoid size, the surface area  
182 of the organoid was measured from the brightfield images on FIJI/ImageJ software, version 1.54f [60].

183 **Immunohistochemistry** – Cortical organoids were fixed in 4% paraformaldehyde (11699408, Q Path) for 2 h at  
184 room temperature (RT) under smooth agitation, followed by three washes of 10 min with Phosphate Buffered  
185 Saline solution (PBS) (18912-014, Gibco) at RT under smooth agitation, and immersed in 30% (v/v) sucrose  
186 (S9378, Sigma-Aldrich) dissolved in PBS for 48 h at 4°C. The organoids were then transferred in a solution  
187 composed of 7.5% (v/v) gelatin (G9391, Sigma-Aldrich) and 15% (v/v) sucrose dissolved in PBS for 1 h at 37°C,  
188 before being embedded in this solution for 15 min at 4°C. Embedded organoids were then snap-frozen in  
189 isopentane (M32631, Sigma-Aldrich) and stored at -80°C until use. Frozen organoids were sectioned in slices of  
190 20 µm thickness using a cryostat (CM1850 UV, Leica Biosystems). For the immunofluorescent staining, organoid  
191 slices were permeabilized and blocked with a solution containing 0.2% Triton® X-100 (T-9284, Sigma-Aldrich),  
192 3% bovine serum albumin (BSA, A2153, Sigma-Aldrich), and 1% normal goat serum (NGS, G9023, Sigma-  
193 Aldrich) in PBS for 1 h at RT. Then, the slices were incubated with primary antibodies diluted in the blocking  
194 solution at 4°C overnight in a humidified chamber and were washed with 0.2% Triton in PBS three times. Then,  
195 organoid slices were incubated with secondary antibodies and 4',6-diamidino-2-phenylindole (DAPI, dilution  
196 1:1000) for 1 h at RT in a dark humidified chamber and were washed three times with 0.2% Triton in PBS. The  
197 slices were mounted using ProLong Gold Antifade Mountant (11539306, Invitrogen), and observed under a Leica  
198 THUNDER microscope (THUNDER Imager Live Cell & 3D Assay, Leica Microsystems). Primary and secondary  
199 antibodies used are listed in Supplementary Table S1.

200 **Image-based quantifications of cellular density and cell-less regions** – Cellular density was calculated based  
201 on DAPI positive surface, without considering cell-less zones (“holes”) since this second parameter was  
202 considered in the subsequent index. Both quantifications of cellular density and cell-less regions relied on  
203 determination of DAPI positive surface and were normalized to the total surface area of the organoid slice. Briefly,  
204 the DAPI positive surface was determined using the “Adjust Threshold” function of FIJI/ImageJ. For the cellular  
205 density, the threshold was adjusted to correspond with the DAPI labelling, while for the cell-less areas, the  
206 threshold was increased to cover the entire surface except the cell-less regions/holes. Estimation of cell number  
207 was calculated based on DAPI positive surface, considering an average nucleus area of 80 µm<sup>2</sup>.

208 **Image-based quantification of GFAP positive surface expression** – Glial Fibrillary Acidic Protein (GFAP)  
209 positive surface expression was calculated using the “Adjust Threshold” function on FIJI/ImageJ, as previously  
210 described in this section, and normalized to the total DAPI positive surface area of the cryosection.

211 **Image-based quantification of γH2AX marker and comparison with a positive control** – Quantification was  
212 conducted by counting γH2AX punctate and by normalizing to the DAPI positive surface expression, across  
213 several sections of individual organoids (n=2-3 slices per organoid, n=4 organoids per condition). Images were  
214 first binarized on FIJI/ImageJ, then the “Analyze Particles” function was applied with the following parameters:  
215 Size (micron2): 15-infinity, Circularity: 0.00-1.00. To statistically compare the maximal γH2AX immunolabelling  
216 in cerebral organoids with positive controls, the standard deviation of the positive controls was first calculated.  
217 Then, the difference between the mean value of the positive controls and the value for the organoids was  
218 determined. Finally, this difference was expressed as a ratio relative to the standard deviation of the positive  
219 controls.

220

## 221 RESULTS

### 222 Quality Control Enables Classification of 60-Day Cortical Organoids by Quality Level

223 We developed a comprehensive QC framework based on a scoring methodology adapted to 60-day  
224 cortical organoid evaluation and classification (Fig. 1). This QC scoring system is structured around five primary  
225 criteria (A to E) corresponding to cortical organoid analysis readouts – A) Morphology, B) Size and growth profile,  
226 C) Cellular composition, D) Cytoarchitectural organization, and E) Cytotoxicity level – each further subdivided  
227 into specific indices (Fig. 1). For each index, cortical organoids are evaluated on a scale of scores between 0 (low  
228 quality) and 5 (high quality). To streamline the process, the criteria are hierarchically organized, prioritizing non-  
229 invasive and critical assessments first (Fig. 1A). Thresholds with minimum scores are defined for each criterion  
230 (Fig. 1B), and failure to meet these thresholds halts further QC evaluation, categorizing the organoid as low-quality  
231 and resulting in its exclusion from the study. In cases where all minimal scores are achieved for a criterion,  
232 additional composite thresholds, integrating multiple indices, are applied to ensure a robust quality classification  
233 (Fig. 1B). For a detailed, illustrated and easy-to-use version of the QC scoring, see Fig. S1 in Supplementary Data.

234 This scoring system is designed for two applications: 1) an Initial QC, which relies exclusively on the  
235 first two non-invasive criteria (A and B) to determine eligibility of the organoids before entering a study (pre-study  
236 QC), and 2) a Final QC based on all the scoring criteria for a complete analysis at the end of a study (post-study  
237 QC) (Fig. 1A). Minimal thresholds have also been determined for passing the Initial and Final QC (Fig. 1B).

238 To validate this QC scoring methodology, we subjected cortical organoids at 60 days of culture to  
239 increasing doses of hydrogen peroxide ( $H_2O_2$ ), a chemical known to induce apoptosis and oxidative stress, to  
240 generate organoids with varying quality levels (Fig. 1C). In this context, organoids were first selected for the  $H_2O_2$   
241 treatment experiment within a batch of cortical organoids, using the Initial QC method.  $H_2O_2$  exposures were  
242 followed by a recovery period of one week, after which the exposed and non-exposed cortical organoids were  
243 evaluated for post-treatment quality using the complete Final QC.

244

## 245 **Initial Quality Control Scoring Streamlines the Selection of Cortical Organoids Based On Non-Invasive 246 Criteria**

247 By day 60 of culture, organoids exhibited spontaneous variability in quality due to the intrinsic  
248 differentiation heterogeneity and stochasticity within organoids (Fig. 2A). Consequently, we evaluated cortical  
249 organoids through the Initial QC based on morphology and size evolutions, to select those eligible for the  $H_2O_2$   
250 exposure experiment. Regarding the morphology evaluation (criterion A), the first index A1 referring to organoid  
251 density and compactness consistently achieved maximum scores of 5/5 across all the organoids (Fig. 2A, 2D). On  
252 the contrary, discrepancies were observed between the organoids for the second index A2 related to border  
253 integrity, with organoid #47 achieving the highest score of 5/5 (Fig. 2Ae, Fig. 2D), organoids #7 and #44 obtaining  
254 a score of 4/5 due to the presence of an area with less-defined border (Fig. 2Aa,d, Fig. 2D), and organoid #29  
255 reaching a low score of 2/5 because of poorly-defined borders, but sufficient to pass the QC index (Fig. 2Ab,  
256 Fig. 2D). However, organoid #31 failed to reach the minimum required score for border integrity (Fig. 2Ac, Fig.  
257 2D), and was excluded from further analysis. Additionally, no cyst formation was observed, allowing all organoids  
258 to pass this third index A3 (Fig. 1A, D).

259 Regarding the organoid sizes and growth evolutions (criterion B), organoids #29 and #44 were excluded  
260 due to insufficient growth both at day 60 and throughout the culture period (Fig. 2B, C, D). Interestingly, organoid  
261 #31 would not have passed this QC step as well but had already been excluded for the first criterion, emphasizing  
262 the relevance of this hierarchical order for QC evaluations. Consequently, only organoids #7 and #47 satisfied the  
263 minimum thresholds for the two non-invasive criteria and successfully passed the Initial QC (Fig. 2D). Overall,  
264 out of 58 cortical organoids generated within this batch, 10 were excluded due to a score lower than 16/25,  
265 representing 17% of the total population.

266

## 267 **Final Quality Control Scoring Effectively Evaluates Cortical Organoids Of Varying Quality Levels**

268 Pre-selected cortical organoids via the Initial QC were included in the  $H_2O_2$  exposure experiment to  
269 generate varying degrees of damage (Fig. 3, S2, S3). A total of six  $H_2O_2$  concentrations were assayed ( $n = 4$   
270 organoids per group): 0% (untreated controls), 0.1%, 0.25%, 0.5%, 1%, and 5%  $H_2O_2$ . Before  $H_2O_2$  exposures, all  
271 the organoids exhibited an optimal morphology, resulting from the Initial QC selection (Fig. 3a1-f1, S2a1-i1, S3a1-  
272 i1). After exposures, organoids exposed to 5% of  $H_2O_2$  displayed severe loss of integrity and cellular  
273 disaggregation (Fig. 3f2, S3g2-i2), thus failing to pass the QC at the morphological criterion for the border integrity  
274 index (Tables 1, S2). This condition also prevented subsequent analyses based on organoid embedding and  
275 sectioning for immunostaining, therefore hampering further QC evaluation for these 5%  $H_2O_2$ -exposed organoids.  
276 Organoids treated with the other  $H_2O_2$  concentrations succeeded to pass the morphology QC according to our  
277 criteria.

278 The size and growth profile criterion were not reassessed post- $H_2O_2$  exposures (Tables 1, S2), as the  
279 seven-day recovery period after  $H_2O_2$  treatment was insufficient for meaningful growth analysis.

280 Subsequent invasive analyses were performed to evaluate cellular composition and cytoarchitectural  
281 organization within the organoids. Immunofluorescence staining confirmed the presence of neural progenitors  
282 (SOX2), immature neurons (TUBB3), and astrocytes (GFAP) across all remaining conditions (Fig. 3a3-e6, S2a3-  
283 i6, S3a3-d6), thus validating the QC criterion of cell type presence verification (Tables 1, S2). However, it must

284 be noted that three organoids (#23, #30 and #47) could not be analyzed by immunolabeling, as they could not be  
285 embedded and sectioned with cryostat, likely due to a lack of compactness. Consequently, these organoids were  
286 excluded at this QC step (Table S2). Interestingly, they belonged to conditions where all the other organoids failed  
287 to pass the QC indices related to cellular composition and cytoarchitectural assessment (Tables 1, S2).

288 Regarding the astrocytic reactivity index, GFAP staining in the remaining organoids treated with 1% H<sub>2</sub>O<sub>2</sub>  
289 (#51 and #53) suggested an excessive astrocytic reactivity, by covering 31% and 22% of the section area,  
290 respectively (Fig. 3e6, S3d6). This implies potential physiological disruption, thus excluding these organoids  
291 according to our QC criteria.

292 The next index evaluates the overall cellular density, based on DAPI staining analysis. Among the  
293 remaining organoids that have passed previous QC steps, we can observe that the cellular density was notably  
294 reduced in organoids exposed with 0.5% H<sub>2</sub>O<sub>2</sub> (#49 and #52), with densities of 6 900 and 7 600 cells.mm<sup>-2</sup>,  
295 respectively (Fig. 3d3, S3b3), therefore not reaching the minimal threshold fixed in the scoring (Fig. S1) and  
296 leading to the exclusion of these organoids.

297 In contrast, no significant cytoarchitectural disruptions – such as the presence of large cell-less regions,  
298 severely altered borders, or occurrence of internal cysts – were observed in the remaining organoids, which  
299 therefore met the QC minimal standards for these criteria (Tables 1, S2). The rosette index was not assessed in this  
300 batch, as neurogenic niches were absent in the control organoids (Tables 1, S2).

301 Finally, cytotoxicity was evaluated via γH2AX staining, a marker of DNA double-stranded breaks, to  
302 quantify DNA damage. For all the remaining organoids exposed to 0%, 0.1% and 0.25% H<sub>2</sub>O<sub>2</sub>, the γH2AX  
303 quantification was significantly different from a positive control of maximal γH2AX labeling (Fig. 3a7-c7, S2a7-  
304 i7), therefore passing this final QC step (Tables 1, S2). Interestingly, all the organoids exposed to higher doses than  
305 0.5% H<sub>2</sub>O<sub>2</sub>, that have been previously excluded at different QC steps, would have failed to pass this final criterion  
306 (Fig. 3d7,e7, S3a7-d7), confirming the validity and relevance of this hierarchical QC system.

307 Overall, Table 2 summarizes the individual final QC scoring results obtained by all the controls and  
308 exposed organoids, as well as the median scores reached per condition. We can observe that the unexposed controls  
309 and organoids exposed to the doses of H<sub>2</sub>O<sub>2</sub> at 0.1% and 0.25% successfully passed the QC. However, organoids  
310 treated with the doses of 0.5%, 1% and 5% H<sub>2</sub>O<sub>2</sub> failed to pass the QC evaluation. We can notice that these excluded  
311 organoids failed at different QC steps, following the hierarchical order of criteria, with 5% H<sub>2</sub>O<sub>2</sub>-exposed  
312 organoids excluded during the morphological criterion, 1% H<sub>2</sub>O<sub>2</sub>-exposed organoids failing regarding the cellular  
313 composition criterion, and 0.5% H<sub>2</sub>O<sub>2</sub>-exposed organoids rejected through either the cytoarchitectural or the  
314 cytotoxicity criteria. Similarly, median scores obtained per condition increase incrementally depending on the  
315 exposure doses, from a low score of 5/50 obtained for the highest dose of H<sub>2</sub>O<sub>2</sub>, up to an elevated score of 47/50  
316 reached for the unexposed controls, thus correlating with the expected damage levels induced by the H<sub>2</sub>O<sub>2</sub> graded  
317 exposures. These results demonstrate the sensitivity of this QC scoring methodology in efficiently and robustly  
318 distinguishing organoid quality levels.

319

## 320 DISCUSSION

321 The stochastic nature of the differentiation of stem cells and their spontaneous self-organization within  
322 cerebral organoids lead to unpredictable variability among them [1]. Novel approaches have recently emerged to  
323 improve culture conditions and enhance organoid reproducibility. For instance, Brain Organoid-on-Chip systems,  
324 which rely on the use of microfluidic devices, offer precise fluid flow control and a more physiologically relevant  
325 microenvironment [45], improving cellular viability [35, 36, 61, 62], neural maturation [61, 63], and organoid  
326 homogeneity [61]. Other advancements include the use of bioreactors, that enable dynamic flow conditions and  
327 enhance oxygenation in large 3D cultures [64–66], as well as bioengineering strategies such as the use of 3D  
328 scaffolds and bioprinting [67–70], which further improve structural consistency. A critical gap remains despite  
329 these innovations: the absence of consensus on what defines high-quality cerebral organoids. This lack of  
330 standardized metrics or guidelines not only hinders meaningful comparisons across studies but also limits the  
331 broader applicability of these models. While complete uniformity should not be the goal, since no living systems  
332 are identical, excessive variability in cerebral organoid quality undermines their predictability and reproducibility,  
333 potentially leading to inaccurate or unreproducible findings, as well as wasted resources. This challenge is further  
334 exacerbated by the absence of standardized protocols for organoid generation, culture and characterization, with

335 numerous in-lab adaptations. As highlighted in a recent publication on a consensus about cerebral organoid  
336 nomenclature [71], there is a pressing need for the establishment of standardized frameworks in the field.  
337 Altogether, this highlights the urgent necessity for a robust and user-friendly quality control framework to ensure  
338 cerebral organoid reliability in both academic and industrial applications.

339 Our scoring-based QC approach, adapted to 60-day cortical organoids, opens the way for a standardized  
340 quality control methodology. By incorporating multiple analysis criteria, including both qualitative macro- and  
341 micro-level observations, this framework provides a complete evaluation to lay the foundation for defining what  
342 constitutes a high-quality cortical organoid. Importantly, our proposed QC is structured hierarchically to rapidly  
343 exclude low-quality organoids, while reserving more detailed analyses for those that passed the initial parameters.  
344 This scoring system enables precise evaluation of each index and criterion using tailored examples and scoring  
345 scales, covering the full quality spectrum observed in cerebral organoids. While morphological criteria remain  
346 qualitative, the clarity and preciseness of the provided examples ensure robust evaluations. These illustrative  
347 examples enhance accessibility, allowing both experts and non-specialists to apply the scoring method effectively.  
348 For the other criteria, quantitative thresholds have been defined. Minimum scores have been established for each  
349 criterion, and failure to meet these scores immediately classifies the organoid as low quality, excluding it from  
350 further evaluations. If all the minimum scores are reached, additional thresholds incorporating multiple indices are  
351 applied to ensure a thorough quality assessment. As an example, for the morphology criterion, minimal scores  
352 required for the three indices are: 3/5 for density, 2/5 for border integrity, and 3/5 for absence of cysts, leading to  
353 a total of 8/15. However, the required minimal total score to pass the morphology criterion is 9/15, implying that  
354 the evaluated organoid could not obtain minimal quality levels for the three indices, and should reach a better  
355 quality for at least one of them (Fig. S1, 1B).

356 We demonstrated the effectiveness and robustness of our QC method through graded H<sub>2</sub>O<sub>2</sub> exposures.  
357 Organoids were initially selected within a batch of cortical organoids for the exposure experiment using the Initial  
358 QC method. After H<sub>2</sub>O<sub>2</sub> exposures, untreated and treated organoids were analyzed using the complete Final QC to  
359 assess post-treatment quality. Overall, the QC results demonstrated that only the untreated organoids exposed to  
360 0.1% and 0.25% H<sub>2</sub>O<sub>2</sub> passed the QC, while those exposed to higher doses above 0.5% did not (Table 2). Median  
361 scores reflected the severity of H<sub>2</sub>O<sub>2</sub> exposure, ranging from a very low QC score (5/50) for the highest dose to an  
362 elevated score (47/50) for controls, correlating with the degree of damage caused by the graded H<sub>2</sub>O<sub>2</sub> exposures.  
363 Importantly, failures occurred at different steps of the hierarchical QC process: organoids exposed to 5%, 1% and  
364 0.5% H<sub>2</sub>O<sub>2</sub> were excluded during the first criterion (morphology), the third criterion (cellular composition), or the  
365 fourth criterion (cytoarchitectures), respectively. These results emphasize the necessity of a stepwise evaluation,  
366 as certain defects are detectable only through deeper cellular or subcellular analysis. Taken together, these  
367 observations demonstrate the precision and reliability of the QC scoring system in differentiating organoid quality  
368 levels.

369 Interestingly, a few recent publications have demonstrated a growing interest in the field of cerebral  
370 organoids for the use of morphological criteria as reliable non-invasive readouts for the characterization of cerebral  
371 organoids [56–58]. Charles and colleagues have implemented a non-invasive quality control system relying on  
372 morphological criteria, enabling the classification of evaluated organoids in high- or low-quality categories for  
373 organoid pre-selection [58]. Remarkably, they integrated brightfield image processing with machine learning tools,  
374 opening the way for automated quality assessment. However, this system is based solely on morphological  
375 observations and does not account for other important analysis criteria that may provide valuable insights beyond  
376 what is visible at the macro-scale. As our study demonstrates, using a scoring scale enables the detection of subtle  
377 variations that a binary classification might overlook. Additionally, the inclusion of parameters such as sphericity  
378 can be questioned, as a brain is inherently far from spherical in shape. Filan et al. have also developed a non-  
379 invasive imaging analysis method for cerebral organoid characterization, also based on brightfield images, and  
380 considering several morphological criteria [56]. Using a 3D quantitative phase imaging technique, they can assess  
381 parameters in a non-invasive manner, such as cellular content, cell morphologies, and rosettes. Similarly, Ikeda  
382 and colleagues have implemented a non-invasive morphological characterization of cerebral organoids combined  
383 with transcriptomic analyses [57]. Interestingly, some analysis criteria are similar to those we selected, such as  
384 verification of transparency level and analysis of cystic structures [57]. Overall, morphological analysis serves as  
385 a valuable initial approach for assessing the quality of cerebral organoids. However, its findings should be validated  
386 through more detailed analyses, which often require invasive techniques.

387 While our proposed scoring system lays a foundation for organoid QC, there are still opportunities for  
388 further refinement and invasive techniques replacement.

389 It is important to note that this scoring system can be applied either manually, as proposed in this study,  
390 or by automation using image processing and machine learning analysis tools, offering flexibility, increased  
391 objectivity, and speed in execution as well as a gain in throughput. Automated analysis could enable organoid  
392 images to be processed and partially scored by the software, reducing variability in evaluations that might arise  
393 from individual interpretation. In particular, the automation could be envisaged primarily for criteria A)  
394 Morphology, based on brightfield images, as demonstrated by Charles and colleagues [58]; and D)  
395 Cytoarchitectures, based on immunofluorescence images.

396 Additionally, incorporating other non-invasive criteria could significantly enhance the transferability of  
397 the scoring system for pre-clinical applications. These could include the detection of specific markers in the  
398 conditioned medium, such as lactate dehydrogenase activity measurement for cytotoxicity evaluation [55],  
399 apoptosis quantification, measurement of reactive oxygen species for oxidative stress analysis, and evaluation of  
400 metabolic activity. While numerous ready-to-use kits are available on the market for these analyses, particular  
401 attention must be paid to the normalization step as these kits are typically designed to be normalized by cell  
402 number, which cannot be easily determined in 3D cultures [55].

403 Regarding the last criterion, which addresses cellular viability and cytotoxicity assessments, we evaluated  
404 DNA damage through  $\gamma$ H2AX immunolabelling. However, other methods could also replace or complete this  
405 example, such as apoptosis detection via cleaved-caspase3 immunolabelling [53], TUNEL assay [52], or  
406 transcriptomic analyses evaluating pro- and anti-apoptotic markers BAX and BCL2 [51]. Ultimately, our  
407 framework provides flexibility, enabling the inclusion or exclusion of parameters based on the specific  
408 characteristics of the study (e.g., neurogenic niches, which could not be assessed here). However, to ensure  
409 consistency, it is crucial to define and validate thresholds through preliminary testing, especially when working  
410 with specific cell lines or different maturation timing. Similarly, growth dynamics should be adjusted according to  
411 the number of cells used during 3D seeding.

412 This QC system holds significant potential for biomedical research, ranging from fundamental to pre-  
413 clinical studies. For neurotoxicity studies, it could facilitate systematic comparisons between exposed and non-  
414 exposed organoids, using consistent scoring across criteria. Similarly, for disease modeling, the scoring system  
415 could be adapted to focus on specific phenotypes critical for recapitulating pathological hallmarks. By addressing  
416 these evolving needs, this framework paves the way for more robust, reproducible, and versatile organoid-based  
417 research. Notably, it represents a critical step toward the much-needed collaborative effort to define and standardize  
418 quality expectations for different types of organoids. As the field moves toward increasingly complex models, such  
419 as assembloids [72], maintaining scientific rigor requires a shared foundation.

420

## 421 REFERENCES

- 422 1. Qian X, Song H, Ming GL (2019) Brain organoids: Advances, applications and challenges. *Development* (Cambridge) 146:. <https://doi.org/10.1242/dev.166074>
- 424 2. Pasca AM, Sloan SA, Clarke LE, et al (2015) Functional cortical neurons and astrocytes from human  
425 pluripotent stem cells in 3D culture. *Nat Methods* 12:671–678. <https://doi.org/10.1038/nmeth.3415>
- 426 3. Susaimanickam PJ, Kiral FR, Park IH (2022) Region Specific Brain Organoids to Study  
427 Neurodevelopmental Disorders. *Int J Stem Cells* 15:26–40. <https://doi.org/10.15283/IJSC22006>
- 428 4. Xiang Y, Tanaka Y, Patterson B, et al (2017) Fusion of regionally-specified hPSC-derived organoids  
429 models human brain development and interneuron migration. *Cell Stel Cell* 21:383–398.  
430 <https://doi.org/10.1016/j.stem.2017.07.007.Fusion>
- 431 5. Xiang Y, Tanaka Y, Cakir B, et al (2019) hESC-derived thalamic organoids form reciprocal projections  
432 when fused with cortical organoids. *Cell Stem Cell* 24:487–497.  
433 <https://doi.org/10.1016/j.stem.2018.12.015.hESC-derived>

- 434 6. Velasco S, Kedaigle AJ, Simmons SK, et al (2019) Individual brain organoids reproducibly form cell  
435 diversity of the human cerebral cortex. *Nature* 570:523–527. <https://doi.org/10.1038/s41586-019-1289-x>
- 436 7. Muguruma K, Nishiyama A, Kawakami H, et al (2015) Self-organization of polarized cerebellar tissue in  
437 3D culture of human pluripotent stem cells. *Cell Rep* 10:537–550.  
438 <https://doi.org/10.1016/j.celrep.2014.12.051>
- 439 8. Sakaguchi H, Kadoshima T, Soen M, et al (2015) Generation of functional hippocampal neurons from self-  
440 organizing human embryonic stem cell-derived dorsomedial telencephalic tissue. *Nat Commun* 6:  
441 <https://doi.org/10.1038/ncomms9896>
- 442 9. Qian Jx, Nguyen HN, Song MM, et al (2016) Brain Region-specific Organoids using Mini-bioreactors for  
443 Modeling ZIKV Exposure. *Cell* 165:1238–1254. <https://doi.org/10.1016/j.cell.2016.04.032>.Brain
- 444 10. Zagare A, Gobin M, Monzel AS, Schwamborn JC (2021) A robust protocol for the generation of human  
445 midbrain organoids. *STAR Protoc* 2:. <https://doi.org/10.1016/j.xpro.2021.100524>
- 446 11. Zivko C, Sagar R, Xydia A, et al (2024) iPSC-derived hindbrain organoids to evaluate escitalopram oxalate  
447 treatment responses targeting neuropsychiatric symptoms in Alzheimer's disease. *Mol Psychiatry*.  
448 <https://doi.org/10.1038/s41380-024-02629-y>
- 449 12. Pellegrini L, Bonfio C, Chadwick J, et al (2020) Human CNS barrier-forming organoids with cerebrospinal  
450 fluid production. *Science* 369:. <https://doi.org/10.1126/SCIENCE.AAZ5626>
- 451 13. Lancaster MA, Renner M, Martin CA, et al (2013) Cerebral organoids model human brain development  
452 and microcephaly. *Nature* 501:373–379. <https://doi.org/10.1038/nature12517>
- 453 14. Wu X, Su J, Wei J, et al (2021) Recent Advances in Three-Dimensional Stem Cell Culture Systems and  
454 Applications. *Stem Cells Int* 2021:. <https://doi.org/10.1155/2021/9477332>
- 455 15. Chiaradia I, Lancaster MA (2020) Brain organoids for the study of human neurobiology at the interface of  
456 in vitro and in vivo. *Nat Neurosci* 23:1496–1508. <https://doi.org/10.1038/s41593-020-00730-3>
- 457 16. Amiri A, Coppola G, Scuderi S, et al (2018) Transcriptome and epigenome landscape of human cortical  
458 development modeled in organoids. *Science* (1979) 362:. <https://doi.org/10.1126/science.aat6720>
- 459 17. Tang XY, Xu L, Wang J, et al (2021) DSCAM/PAK1 pathway suppression reverses neurogenesis deficits  
460 in iPSC-derived cerebral organoids from patients with down syndrome. *Journal of Clinical Investigation*  
461 131:. <https://doi.org/10.1172/JCI135763>
- 462 18. Xu R, Brawner AT, Li S, et al (2019) OLIG2 Drives Abnormal Neurodevelopmental Phenotypes in Human  
463 iPSC-Based Organoid and Chimeric Mouse Models of Down Syndrome. *Cell Stel Cell* 24:908–926.  
464 [https://doi.org/10.1016/j.stem.2019.04.014.OLIG2](https://doi.org/10.1016/j.stem.2019.04.014)
- 465 19. Alić I, Goh PA, Murray A, et al (2021) Patient-specific Alzheimer-like pathology in trisomy 21 cerebral  
466 organoids reveals BACE2 as a gene dose-sensitive AD suppressor in human brain. *Mol Psychiatry*  
467 26:5766–5788. <https://doi.org/10.1038/s41380-020-0806-5>
- 468 20. Bian S, Repic M, Guo Z, et al (2018) Genetically engineered cerebral organoids model brain tumour  
469 formation. *Nat Methods* 15:631–639. <https://doi.org/10.1038/s41592-018-0070-7.Genetically>
- 470 21. Nassor F, Jarray R, Biard DSF, et al (2020) Long Term Gene Expression in Human Induced Pluripotent  
471 Stem Cells and Cerebral Organoids to Model a Neurodegenerative Disease. *Front Cell Neurosci* 14:1–7.  
472 <https://doi.org/10.3389/fncel.2020.00014>
- 473 22. Pavoni S, Jarray R, Nassor F, et al (2018) Small-molecule induction of Aβ-42 peptide production in human  
474 cerebral organoids to model Alzheimer's disease associated phenotypes. *PLoS One* 13:1–15.  
475 <https://doi.org/10.1371/journal.pone.0209150>
- 476 23. Kim H, Park HJ, Choi H, et al (2019) Modeling G2019S-LRRK2 Sporadic Parkinson's Disease in 3D  
477 Midbrain Organoids. *Stem Cell Reports* 12:518–531. <https://doi.org/10.1016/j.stemcr.2019.01.020>

- 478 24. Groveman BR, Foliaki ST, Orru CD, et al (2019) Sporadic Creutzfeldt-Jakob disease prion infection of  
479 human cerebral organoids. *Acta Neuropathol Commun* 7:90. <https://doi.org/10.1186/s40478-019-0742-2>
- 480 25. Giorgi C, Lombardozzi G, Ammannito F, et al (2024) Brain Organoids: A Game-Changer for Drug Testing.  
481 *Pharmaceutics* 16
- 482 26. Zhou JQ, Zeng LH, Li CT, et al (2023) Brain organoids are new tool for drug screening of neurological  
483 diseases. *Neural Regen Res* 18:1884–1889
- 484 27. Cui K, Wang Y, Zhu Y, et al (2020) Neurodevelopmental impairment induced by prenatal valproic acid  
485 exposure shown with the human cortical organoid-on-a-chip model. *Microsyst Nanoeng* 6:.  
486 <https://doi.org/10.1038/s41378-020-0165-z>
- 487 28. Zang Z, Yin H, Du Z, et al (2022) Valproic acid exposure decreases neurogenic potential of outer radial  
488 glia in human brain organoids. *Front Mol Neurosci* 15:. <https://doi.org/10.3389/fnmol.2022.1023765>
- 489 29. Meng Q, Zhang W, Wang X, et al (2022) Human forebrain organoids reveal connections between valproic  
490 acid exposure and autism risk. *Transl Psychiatry* 12:. <https://doi.org/10.1038/s41398-022-01898-x>
- 491 30. Rhinn M, Zapata-Bodalo I, Klein A, et al (2022) Aberrant induction of p19Arf-mediated cellular  
492 senescence contributes to neurodevelopmental defects. *PLoS Biol* 20:.  
493 <https://doi.org/10.1371/journal.pbio.3001664>
- 494 31. Yokoi R, Nagafuku N, Ishibashi Y, et al (2023) Contraindicated Drug Responses in Dravet Syndrome Brain  
495 Organoids Utilizing Micro Electrode Array Assessment Methods. *Organoids* 2:177–191.  
496 <https://doi.org/10.3390/organoids2040014>
- 497 32. Takla TN, Luo J, Sudyk R, et al (2023) A Shared Pathogenic Mechanism for Valproic Acid and SHROOM3  
498 Knockout in a Brain Organoid Model of Neural Tube Defects. *Cells* 12:.  
499 <https://doi.org/10.3390/cells12131697>
- 500 33. Tidball AM, Niu W, Ma Q, et al (2023) Deriving early single-rosette brain organoids from human  
501 pluripotent stem cells. *Stem Cell Reports* 18:2498–2514. <https://doi.org/10.1016/j.stemcr.2023.10.020>
- 502 34. Lee JH, Shaker MR, Park SH, Sun W (2023) Transcriptional Signature of Valproic Acid-Induced Neural  
503 Tube Defects in Human Spinal Cord Organoids. *Int J Stem Cells* 16:385–393.  
504 <https://doi.org/10.15283/IJSC23012>
- 505 35. Wang Y, Wang L, Zhu Y, Qin J (2018) Human brain organoid-on-a-chip to model prenatal nicotine  
506 exposure. *Lab Chip* 18:851–860. <https://doi.org/10.1039/c7lc01084b>
- 507 36. Ao Z, Cai H, Havert DJ, et al (2020) One-Stop Microfluidic Assembly of Human Brain Organoids to  
508 Model Prenatal Cannabis Exposure. *Anal Chem* 92:4630–4638.  
509 <https://doi.org/10.1021/acs.analchem.0c00205>
- 510 37. Abdulla A, Yan H, Chen S, et al (2025) A multichannel microfluidic device for revealing the neurotoxic  
511 effects of Bisphenol S on cerebral organoids under low-dose constant exposure. *Biosens Bioelectron*  
512 267:116754. <https://doi.org/10.1016/J.BIOS.2024.116754>
- 513 38. Cao Y, Hu D, Cai C, et al (2023) Modeling early human cortical development and evaluating neurotoxicity  
514 with a forebrain organoid system. *Environmental Pollution* 337:.  
515 <https://doi.org/10.1016/j.envpol.2023.122624>
- 516 39. Hu D, Cao Y, Cai C, et al (2025) Establishment of human cerebral organoid systems to model early neural  
517 development and assess the central neurotoxicity of environmental toxins. *Neural Regen Res* 20:242–252.  
518 <https://doi.org/10.4103/nrr.nrr-d-23-00928>
- 519 40. Chen S, Chen Y, Gao Y, et al (2023) Toxic effects and mechanisms of nanoplastics on embryonic brain  
520 development using brain organoids model. *Science of the Total Environment* 904:.  
521 <https://doi.org/10.1016/j.scitotenv.2023.166913>

- 522 41. Yao H, Hu D, Wang J, et al (2023) Buprenorphine and methadone differentially alter early brain  
523 development in human cortical organoids. *Neuropharmacology* 239:.  
524 <https://doi.org/10.1016/j.neuropharm.2023.109683>
- 525 42. Acharya P, Shrestha S, Joshi P, et al (2024) Dynamic culture of cerebral organoids using a pillar/perfusion  
526 plate for the assessment of developmental neurotoxicity
- 527 43. Liu Z, Wang Z, Wei Y, et al (2023) Transcriptomic Profiling of Tetrodotoxin-Induced Neurotoxicity in  
528 Human Cerebral Organoids. *Mar Drugs* 21:. <https://doi.org/10.3390/md21110588>
- 529 44. Tian C, Cai H, Ao Z, et al (2024) Engineering human midbrain organoid microphysiological systems to  
530 model prenatal PFOS exposure. *Science of The Total Environment* 947:174478.  
531 <https://doi.org/10.1016/J.SCITOTENV.2024.174478>
- 532 45. Castiglione H, Vigneron PA, Baquerre C, et al (2022) Human Brain Organoids-on-Chip: Advances,  
533 Challenges, and Perspectives for Preclinical Applications. *Pharmaceutics* 14
- 534 46. Giandomenico SL, Sutcliffe M, Lancaster MA (2021) Generation and long-term culture of advanced  
535 cerebral organoids for studying later stages of neural development. *Nat Protoc* 16:579–602.  
536 <https://doi.org/10.1038/s41596-020-00433-w>
- 537 47. Lancaster MA, Knoblich JA (2014) Generation of Cerebral Organoids from Human Pluripotent Stem  
538 Cells. *Nature Protocol* 9:2329–2340. <https://doi.org/10.1038/nprot.2014.158.Generation>
- 539 48. Kang YJ, Cho H (2021) Human brain organoids in Alzheimer’s disease. *Organoid* 1:e5.  
540 <https://doi.org/10.51335/organoid.2021.1.e5>
- 541 49. Quadrato G, Nguyen T, Macosko EZ, et al (2017) Cell diversity and network dynamics in photosensitive  
542 human brain organoids. *Nature* 545:48–53. <https://doi.org/10.1038/nature22047>
- 543 50. Schröter M, Wang C, Terrigno M, et al (2022) Functional imaging of brain organoids using high-density  
544 microelectrode arrays. *MRS Bull* 47:530–544. <https://doi.org/10.1557/s43577-022-00282-w>
- 545 51. Basu A, Haldar S (1998) The relationship between Bcl2, Bax and p53: consequences for cell cycle  
546 progression and cell death. *Mol Hum Reprod* 4:1099–1109
- 547 52. Loo DT (2011) In situ detection of apoptosis by the TUNEL assay: An overview of techniques. *Methods*  
548 in Molecular Biology
- 682:3–13. [https://doi.org/10.1007/978-1-60327-409-8\\_1](https://doi.org/10.1007/978-1-60327-409-8_1)
- 549 53. Bressenot A, Marchal S, Bezdetnaya L, et al (2009) Assessment of Apoptosis by Immunohistochemistry  
550 to Active Caspase-3, Active Caspase-7, or Cleaved PARP in Monolayer Cells and Spheroid and  
551 Subcutaneous Xenografts of Human Carcinoma. *Journal of Histochemistry and Cytochemistry* 57:289–  
552 300. <https://doi.org/10.1369/jhc.2008.952044>
- 553 54. Podhorecka M, Skladanowski A, Bozko P (2010) H2AX Phosphorylation: Its Role in DNA Damage  
554 Response and Cancer Therapy. *J Nucleic Acids* 2010:1–9. <https://doi.org/10.4061/2010/920161>
- 555 55. Castiglione H, Madrange L, Lemonnier T, et al (2024) Development and Optimization of a Lactate  
556 Dehydrogenase Assay Adapted to 3D Cell Cultures. *Organoids* 3:113–125.  
557 <https://doi.org/10.3390/organoids3020008>
- 558 56. Filan C, Charles S, Casteleiro Costa P, et al (2024) Non-invasive label-free imaging analysis pipeline for  
559 in situ characterization of 3D brain organoids. *Sci Rep* 14:22331. [https://doi.org/10.1038/s41598-024-72038-2](https://doi.org/10.1038/s41598-024-<br/>560 72038-2)
- 561 57. Ikeda M, Doi D, Ebise H, et al (2024) Validation of non-destructive morphology-based selection of  
562 cerebral cortical organoids by paired morphological and single-cell RNA-seq analyses. *Stem Cell Reports*.  
563 <https://doi.org/10.1016/j.stemcr.2024.09.005>
- 564 58. Charles S, Jackson-Holmes E, Sun G, et al (2024) Non-Invasive Quality Control of Organoid Cultures  
565 Using Mesofluidic CSTR Bioreactors and High-Content Imaging

- 566 59. Temple J, Velliou E, Shehata M, Lévy R (2022) Current strategies with implementation of three-  
567 dimensional cell culture: the challenge of quantification. Interface Focus 12:.  
568 <https://doi.org/10.1098/rsfs.2022.0019>
- 569 60. Schindelin J, Arganda-Carreras I, Frise E, et al (2012) Fiji: An open-source platform for biological-image  
570 analysis. Nat Methods 9:676–682. <https://doi.org/10.1038/nmeth.2019>
- 571 61. Cho AN, Jin Y, An Y, et al (2021) Microfluidic device with brain extracellular matrix promotes structural  
572 and functional maturation of human brain organoids. Nat Commun 12:. <https://doi.org/10.1038/s41467-021-24775-5>
- 574 62. Wang Y, Wang L, Guo Y, et al (2018) Engineering stem cell-derived 3D brain organoids in a perfusable  
575 organ-on-a-chip system. RSC Adv 8:1677–1685. <https://doi.org/10.1039/c7ra11714k>
- 576 63. Karzbrun E, Kshirsagar A, Cohen SR, et al (2018) Human brain organoids on a chip reveal the physics of  
577 folding. Nat Phys 14:515–522. <https://doi.org/10.1038/s41567-018-0046-7>
- 578 64. Grün C, Altmann B, Gottwald E (2020) Advanced 3d cell culture techniques in micro-bioreactors, Part I:  
579 A systematic analysis of the literature published between 2000 and 2020. Processes 8:1–24
- 580 65. Altmann B, Grün C, Nies C, Gottwald E (2020) Advanced 3D Cell Culture Techniques in Micro-  
581 Bioreactors, Part II: Systems and Applications. Processes 9:21. <https://doi.org/10.3390/pr9010021>
- 582 66. Qian X, Jacob F, Song MM, et al (2018) Generation of human brain region-specific organoids using a  
583 miniaturized spinning bioreactor. Nat Protoc 13:565–580. <https://doi.org/10.1038/nprot.2017.152>
- 584 67. Garreta E, Kamm RD, Chuva de Sousa Lopes SM, et al (2021) Rethinking organoid technology through  
585 bioengineering. Nat Mater 20:145–155
- 586 68. Hofer M, Lutolf MP (2021) Engineering organoids. Nat Rev Mater 6:402–420
- 587 69. Cadena MA, Sing A, Taylor K, et al (2024) A 3D Bioprinted Cortical Organoid Platform for Modeling  
588 Human Brain Development. Adv Healthc Mater. <https://doi.org/10.1002/adhm.202401603>
- 589 70. Roth JG, Brunel LG, Huang MS, et al (2023) Spatially controlled construction of assembloids using  
590 bioprinting. Nat Commun 14:. <https://doi.org/10.1038/s41467-023-40006-5>
- 591 71. Paşa SP, Arlotta P, Bateup HS, et al (2022) A nomenclature consensus for nervous system organoids and  
592 assembloids. 609:907–910. <https://doi.org/10.1038/s41586-022-05219-6>
- 593 72. Miura Y, Li MY, Revah O, et al (2022) Engineering brain assembloids to interrogate human neural circuits.  
594 Nat Protoc 17:15–35
- 595

## 596 STATEMENTS & DECLARATIONS

### 597 Funding

598 The authors declare that no funds, grants, or other support were received during the preparation of this manuscript.

### 599 Competing Interests

600 Financial interests: Héloïse Castiglione, Camille Baquerre, Benoît Guy Christian Maisonneuve, Jessica Rontard  
601 and Thibault Honegger are employed by NETRI company, whose CEO is Thibault Honegger.

### 602 Author Contributions

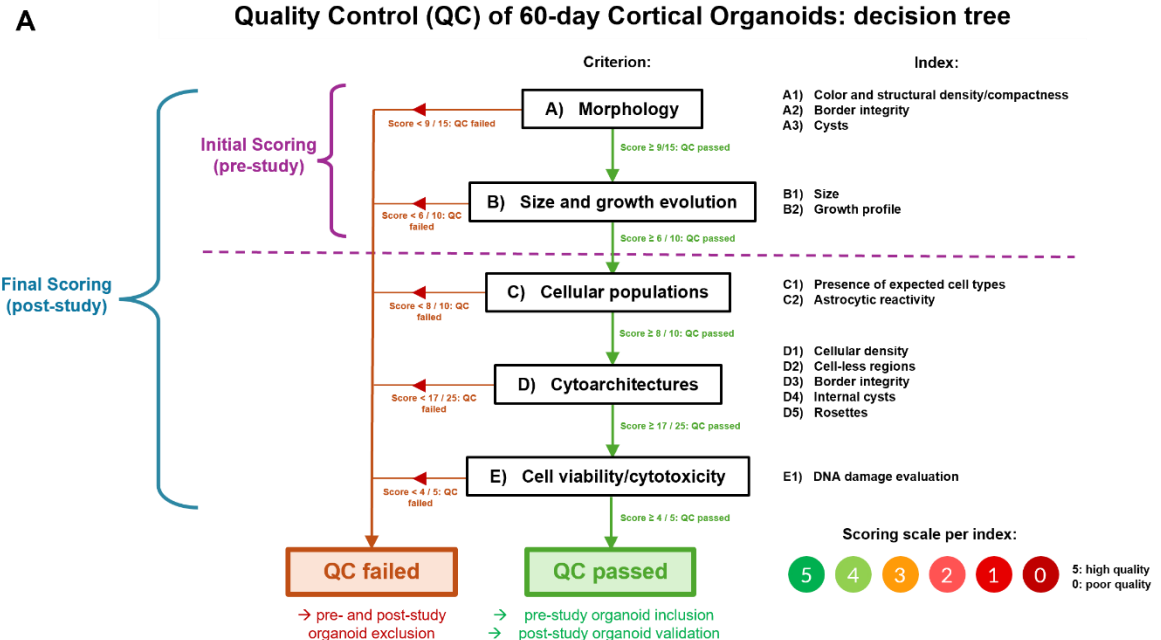
603 All authors contributed to the study conception and design. Material preparation, data collection and analysis were  
604 performed by Héloïse Castiglione, Lucie Madrange, Camille Baquerre, Jessica Rontard and Pierre-Antoine  
605 Vigneron. The first draft of the manuscript was written by Héloïse Castiglione, Jessica Rontard and Pierre-Antoine  
606 Vigneron and all authors commented on previous versions of the manuscript. All authors read and approved the  
607 final manuscript.

608 **Data Availability**

609 The data underlying this article will be shared on reasonable request to the corresponding authors.

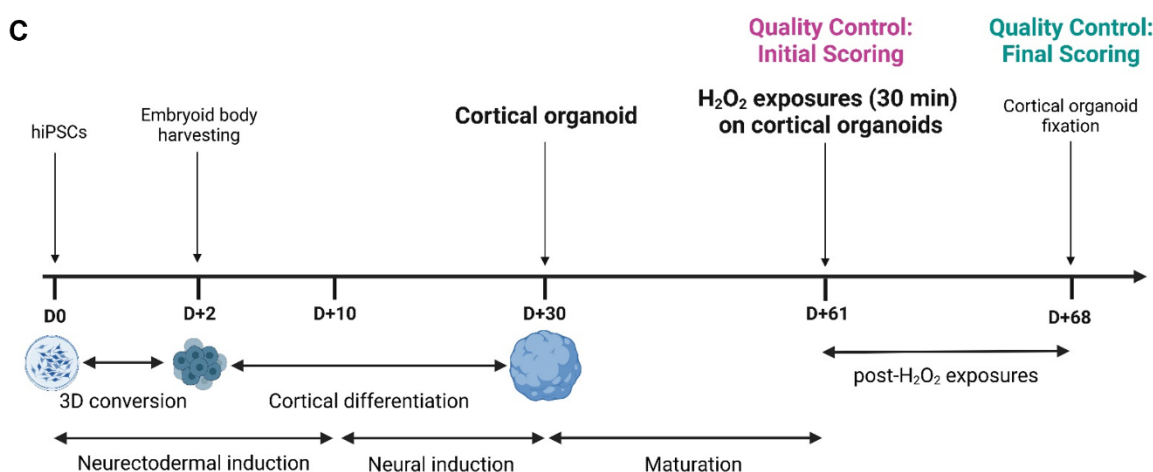
610

611 **FIGURES & LEGENDS**



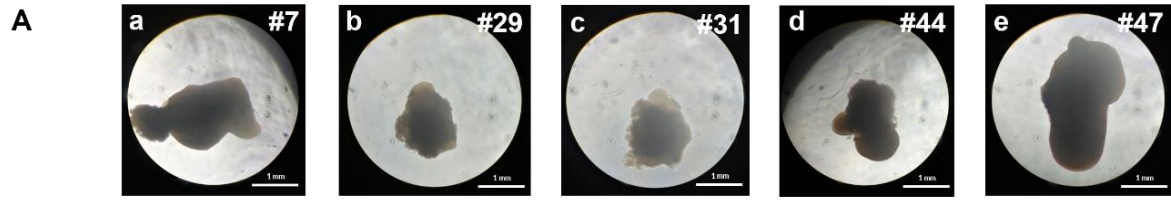
**B**

Criterion	Index	Analytical method	Minimal score required / index	Minimal score required / readout or group of indices	Minimal score required (when all criteria are passed)	Initial Scoring (pre-study)	Final Scoring (post-study)	
<b>A) Morphology</b>	<u>A1) Color and structural density / compactness</u>		3 / 5					
	<u>A2) Border integrity</u>	Brightfield microscopy	2 / 5	9 / 15				
	<u>A3) Cysts</u>		3 / 5			16 / 25		
<b>B) Size and growth evolution</b>	<u>B1) Size</u>	Area measurement	3 / 5	6 / 10				
	<u>B2) Growth profile</u>		3 / 5					
<b>C) Cellular populations</b>	<u>C1) Presence of expected cell types</u>	Immunohistochemistry	4 / 5	8 / 10				
	<u>C2) Astrocytic reactivity</u>	Transcriptomics	4 / 5			45 / 65		
<b>D) Cytoarchitectures</b>	<u>D1) Cellular density</u>		3 / 5					
	<u>D2) Cell-less regions</u>		3 / 5	7 / 10				
	<u>D3) Border integrity</u>	Immunohistochemistry	3 / 5	14 / 20			17 / 25	
	<u>D4) Internal cysts</u>		3 / 5					
<u>D5) Rosettes (if applicable)</u>		3 / 5						
<b>E) Cell viability / cytotoxicity</b>	<u>E1) DNA damage evaluation</u>	Immunohistochemistry	4 / 5	4 / 5				



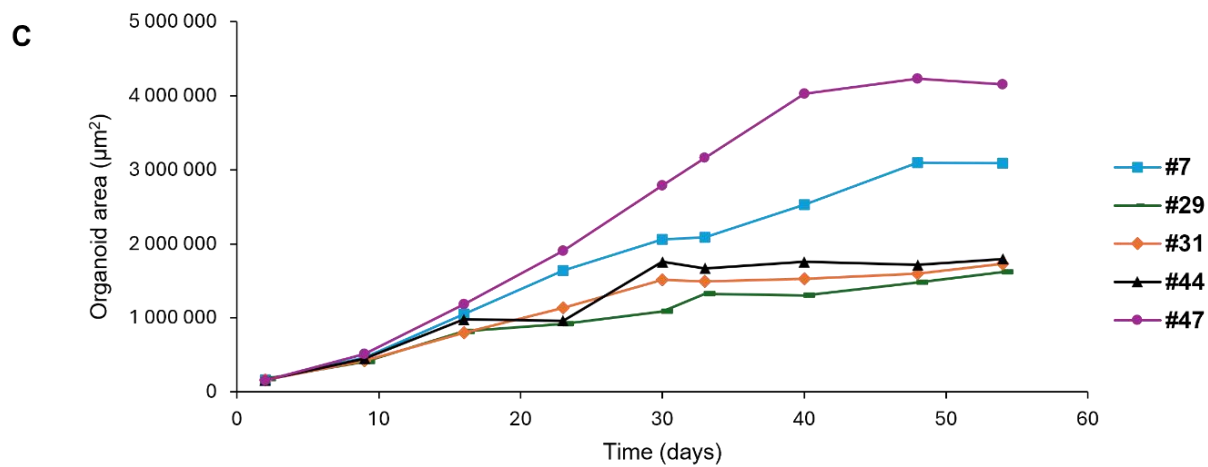
612

613     **Fig. 1:** Overview of Quality Control methodology for 60-day cortical organoids, and validation by scoring of H<sub>2</sub>O<sub>2</sub>-exposed cortical  
614     organoids. (A) Overview of the Quality Control (QC) adapted to 60-day cortical organoids. The QC relies on several criteria, subdivided into  
615     indices, for cortical organoid analysis, including Morphology, Size and growth profile, Presence of expected cellular populations at 60 days,  
616     Cytoarchitectural organization, and Cellular viability and cytotoxicity levels. For each index, a scoring system enables the evaluation of  
617     organoids based on the attribution of scores comprised between 0 (poor quality) and 5 (high quality). The QC follows a hierarchical structure:  
618     criteria are assessed sequentially, and failure to meet an initial criterion automatically classifies the organoid as low quality and subsequent  
619     criteria are not assessed. The scoring system is divided into two QC: 1) an Initial Scoring to select cortical organoids before entering a study,  
620     based on the two first non-invasive criteria Morphology and Growth; and 2) a Final Scoring for complete analysis of cortical organoids based  
621     on all the criteria at the end of a study. (B) Summary table of QC criteria and minimal scores required per indices, and per composite groups  
622     of indices and readouts, that have to be obtained for cortical organoids to pass the QC. (C) Timeline of cortical organoid generation and culture  
623     protocols, including an overview of H<sub>2</sub>O<sub>2</sub> exposure conditions. Before H<sub>2</sub>O<sub>2</sub> exposure at D+61, cortical organoids were selected based on the  
624     Initial Scoring for QC. Exposed cortical organoids at D+68 were then evaluated following the Final Scoring for complete QC



**B**

	Organoid number				
Organoid size: area ( $\mu\text{m}^2$ )	#7	#29	#31	#44	#47
Day 10	465 499	408 551	397 689	451 789	514 644
Day 30	2 061 307	1 088 069	1 419 349	1 755 713	2 789 299
Day 60	3 088 813	1 615 435	1 733 997	1 796 685	4 153 616
Linear regression's slope	60 327	26 986	30 503	32 953	88 615

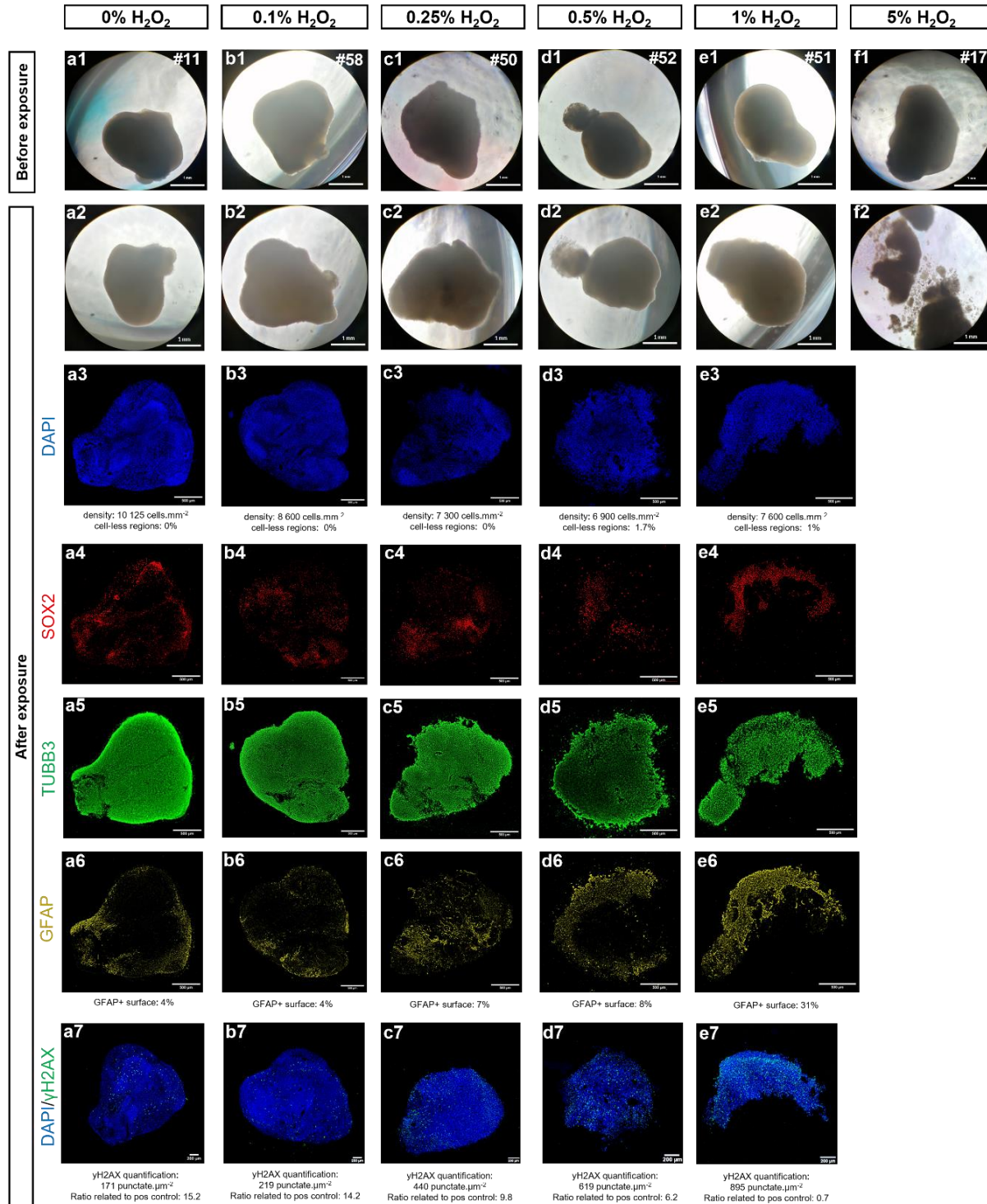


**D Scoring recapitulative table of organoid examples for Initial QC**

Organoid number	A) Morphology			B) Size and growth		Total score / 25	QC Initial Scoring result
	A1) Density	A2) Border integrity	A3) Cysts	B1) Size	B2) Growth		
	Minimal score	3 / 5	2 / 5	3 / 5	3 / 5		
#7	5	4	5	4	4	22	Passed
#29	5	2	5	1 → QC failed	x	13	Failed
#31	5	1 → QC failed	x	x	x	6	Failed
#44	5	4	5	1 → QC failed	x	15	Failed
#47	5	5	5	5	4	24	Passed

626  
627  
628  
629  
630  
631

**Fig. 2:** Quality Control (QC) for selection of cortical organoids before the H<sub>2</sub>O<sub>2</sub> exposure experiment, following the Initial Scoring based on the first two non-invasive criteria Morphology and Growth evolutions. (A) Morphology of example cortical organoids within a batch at 60 days of culture (brightfield, 5X). (B) Table summarizing organoid sizes as surface areas at three timepoints of interest (Day 10, Day 30, and Day 60), as well as corresponding linear regression's slopes. (C) Growth curves of individual organoids from D+2 to D+60 of culture. (D) Recapitulative table of scores obtained by the example organoids for each readout and indices of the Initial QC. Minimal scores per indices and the total minimal score required for Initial QC validation are mentioned. Results of QC for each organoid are indicated as Passed/Failed



632

633 **Fig. 3:** Quality Control (QC) for evaluation of cortical organoids after H<sub>2</sub>O<sub>2</sub> exposures, following the Final Scoring based on all the  
634 criteria. H<sub>2</sub>O<sub>2</sub> exposures on cortical organoids serve as examples of varying organoid quality levels through incremental H<sub>2</sub>O<sub>2</sub> doses, with  
635 examples of organoids passing or not the QC. (a1-f1) Examples of cortical organoids exposed to different H<sub>2</sub>O<sub>2</sub> doses comprised between 0%  
636 and 5%. Morphology before (a1-f1) and after (a2-f2) H<sub>2</sub>O<sub>2</sub> exposures serve to evaluate the first criterion related to morphological quality  
637 evaluation (brightfield, 5X). Immunofluorescent staining of the example organoids for DAPI (a3-e3), neural progenitor marker SOX2 (a4-e4),  
638 neuronal marker TUBB3 (a5-e5), and astrocytic marker GFAP (a6-e6) enable the assessment of the following criteria: verification of cell types  
639 presence, assessment of Astrocytic reactivity, and evaluation of Cytoarchitectural organization. Immunofluorescent labeling of DNA damage  
640 with γH2AX marker enables evaluation of Cytotoxicity level (a7-e7) (Leica THUNDER microscope, 20X)

641 **Table 1: Scoring recapitulative table of H<sub>2</sub>O<sub>2</sub>-exposed organoid examples for Final QC**

H <sub>2</sub> O <sub>2</sub> dose	Organoid number	A) Morphology			B) Size and Growth		C) Cellular populations		D) Cytoarchitectural organization					E) Cellular viability / Cytotoxicity	Total score	QC Final Scoring result
		A1) Density	A2) Border integrity	A3) Cysts	B1) Size	B2) Growth	C1) Expected cell types	C2) Astrocytic reactivity	D1) Cellular density	D2) Cell-less regions	D3) Border integrity	D4) Internal cysts	D5) Rosette	E1) DNA damage		
		Minimal score														
		3 / 5	2 / 5	3 / 5	3 / 5	3 / 5	4 / 5	4 / 5	3 / 5	3 / 5	3 / 5	3 / 5	3 / 5	4 / 5	35 / 50	
0%	#11	5	5	5	NA	NA	5	5	5	5	5	5	NA	5	50	Passed
0.1%	#58	5	5	4			5	5	3	5	5	5		5	47	Passed
0.25%	#50	5	5	5			5	5	3	5	3	5		4	45	Passed
0.5%	#52	5	4	5			5	5	0 → QC failed	x	x	x		x	24	Failed
1%	#51	5	3	5			5	0 → QC failed	x	x	x	x		x	18	Failed
5%	#17	3	0 → QC failed	x			x	x	x	x	x	x		x	3	Failed

642

643 Recapitulative table of scores for H<sub>2</sub>O<sub>2</sub>-exposed organoid examples through Final QC. Individual scores obtained for each criterion and indices of the QC are indicated, as well as minimal scores required for QC validation.  
644 Results of QC for each organoid are indicated as Passed / Failed QC

645 **Table 2: Recapitulative table of final QC scores obtained for H<sub>2</sub>O<sub>2</sub>-exposed cortical organoids**

H <sub>2</sub> O <sub>2</sub> dose	Organoid number	Individual QC total score / 50	Median QC total score / 50	QC result	Step of exclusion		
		Minimal score					
		35 / 50	35 / 50				
0% control	#11	50	47	Passed			
	#41	47					
	#57	47					
	#59	47					
0.1%	#21	45	46	Passed			
	#37	48					
	#55	45					
	#58	47					
0.25%	#8	45	44	Passed			
	#36	45					
	#48	43					
	#50	45					
0.5%	#16	40	15	Failed	D) Cytoarchitectures D1) Cellular density E) Cytotoxicity E1) DNA damage		
	#30	12					
	#49	15					
	#52	24					
1%	#23	14	14	Failed	C) Cellular populations C2) Astrocytic reactivity		
	#47	14					
	#51	18					
	#53	20					
5%	#17	3	5	Failed	A) Morphology A2) Border integrity		
	#20	6					
	#32	5					
	#46	6					

646 Individual final scores obtained by the H<sub>2</sub>O<sub>2</sub>-exposed organoids for each criterion and indices of the QC are indicated, along with minimum  
647 scores required for QC validation. Median scores obtained per H<sub>2</sub>O<sub>2</sub> dose conditions are also mentioned, as well as whether the organoids have  
648 passed or failed the QC. For those who have failed the QC, the scoring step at which they have been excluded is specified